Neuron, Vol. 37, 333–346, January 23, 2003, Copyright ©2003 by Cell Press

Integration of Local Features into Global Shapes: Monkey and Human fMRI Studies

Zoe Kourtzi,* Andreas S. Tolias, Christian F. Altmann, Mark Augath, and Nikos K. Logothetis
Max Planck Institute for Biological Cybernetics
72076 Tuebingen
Germany

Summary

The integration of local image features into global shapes was investigated in monkeys and humans using fMRI. An adaptation paradigm was used, in which stimulus selectivity was deduced by changes in the course of adaptation of a pattern of randomly oriented elements. Accordingly, we observed stronger activity when orientation changes in the adapting stimulus resulted in a collinear contour than a different random pattern. This selectivity to collinear contours was observed not only in higher visual areas that are implicated in shape processing, but also in early visual areas where selectivity depended on the receptive field size. These findings suggest that unified shape perception in both monkeys and humans involves multiple visual areas that may integrate local elements to global shapes at different spatial scales.

Introduction

A fundamental question in visual perception is how local image features are integrated into global configurations and perceived as visual shapes. Traditionally, the visual system is thought to be hierarchically organized (Felleman and Van Essen, 1991; Van Essen et al., 1992) in early visual areas (V1, V2, V3, V4) that are involved in the analysis of simple local features (Hubel and Wiesel, 1968) and in higher visual areas (regions in the inferotemporal cortex) that are implicated in the processing of complex global shapes (Maunsell and Newsome, 1987, for review). Recently, there is accumulating evidence that early visual areas (e.g., V1, V2) may respond to global rather than simple local features (Gilbert, 1992, 1998; Allman et al., 1985; Lamme et al., 1998; Fitzpatrick, 2000, for reviews). Comparing findings across these studies and drawing conclusions about the role of different visual areas in the unified perception of shapes is not possible because (1) different types of stimuli have been used across studies to test responses in different visual areas (i.e., edges or contours for early visual areas versus complex objects for higher visual areas), and (2) the electrophysiological techniques used in these studies recorded from single rather than multiple visual areas simultaneously. As a result, the question of how the unified perception of a global shape or a "good Gestalt" (Kofka, 1935) emerges from the output of local feature detectors remains open. The aim of this study was to test the role of both early and higher visual areas in the integration of local features into global shapes.

To this end, we conducted functional magnetic resonance imaging (fMRI) studies. Although fMRI lacks the high spatial resolution of intracortical recordings, it allows simultaneous collection of responses to the same stimulus set from multiple visual areas that is not possible with standard recording techniques. We performed these studies in monkeys, where much is known about the properties of neurons in different visual areas (Hubel and Wiesel, 1968; Felleman and Van Essen, 1991; Van Essen et al., 1992), and in humans, where recent fMRI studies provide evidence for functional organization of the visual cortex (Wandell, 1999, for review). The strong correlation between the fMRI signal and the underlying neural responses (Logothetis et al., 2001) emphasizes the importance of such studies for bridging the gap between the extensive neurophysiological findings in monkeys and those reported in combined psychophysical and imaging investigations with humans. Our goal was to investigate the visual integration processes in both the monkey and the human brain by using the same fMRI technique and similar experimental paradigms.

We tested responses across visual areas to collinear contours versus random patterns. The collinear patterns consisted of a number of similarly oriented elements embedded into a background of randomly oriented elements, while the random patterns consisted of a field of randomly oriented elements. Such displays yield the perception of a global figure in a randomly textured background (Figures 1 and 5) and are thought to emerge from a segmentation process relying on the integration of the similarly oriented line segments into global configurations (Field et al., 1993; Hess and Field, 1999, for review; Kovacs and Julesz, 1993, 1994).

To test the selectivity to collinear rather than random patterns across visual areas, we employed a neural adaptation paradigm that capitalizes on the reduction of neural responses for stimuli that have been presented for prolonged time or repeatedly. A change in a specific stimulus dimension that elicits increased responses (i.e., rebound of activity) identifies neural populations that are tuned to the modified stimulus attributes. This paradigm has been used in both monkey (Tolias et al., 2001) and human (Buckner et al., 1998; Grill-Spector et al., 1999; Kourtzi and Kanwisher, 2000, 2001) fMRI studies as a sensitive tool that allows us to investigate the selectivity of the neural populations within the imaged voxels. This is not possible with conventional fMRI paradigms that rely on the subtraction of activation between different stimulus types since they average across neural populations that may respond homogeneously across stimulus changes or may be differentially tuned to different stimulus attributes. For example, it is possible that collinear and random patterns are encoded by different neural populations but at a finer spatial resolution than the measured voxels. In this case, higher sensitivity to collinear than random patterns is most likely to be detectable by adaptation measures rather than subtraction methods.

In the present study, we used a random pattern as

*Correspondence: zoe.kourtzi@tuebingen.mpg.de

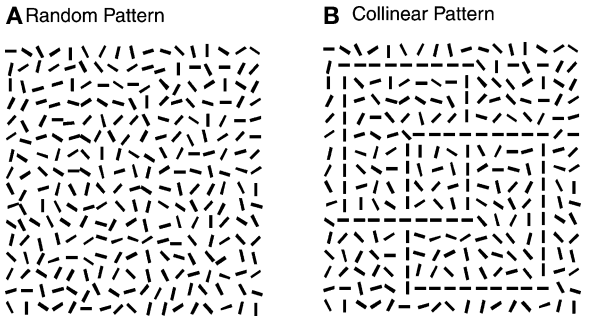

Figure 1. Stimuli for the Monkey fMRI Adaptation Study

(A) Random pattern used as the adapting stimulus.

(B) Collinear pattern used as the test stimulus.

the adapting stimulus that was followed by one of three test stimuli: (1) a random pattern identical to the adapting stimulus, (2) a different random pattern different from the adapting stimulus generated by changing randomly the orientation of some of the elements, and (3) a collinear pattern in which changes in the orientation of the local elements resulted in a collinear contour. Decreased responses when the test stimulus was identical to the adapting stimulus would indicate the basic adaptation effect. Rebound of activity for a random pattern different from the adapting stimulus would suggest regions involved in the processing of local orientation. More interestingly, stronger rebound effects for collinear than for random patterns would indicate regions involved selectively in the processing of global contours rather than local orientation. Our monkey and human fMRI studies showed selective responses to collinear rather than random patterns in both early and higher visual areas. Interestingly, these selective responses to collinear contours differed across the early visual areas based on their receptive field (RF) size. These findings suggest that multiple visual areas are involved in the integration of local elements to global shapes at different spatial scales.

Results

Monkey fMRI Studies

The stimuli used were either randomly oriented line segments appearing as formless texture or patterns (e.g., cube) generated by approximately collinear stimulus line segments embedded in a field of randomly oriented ones (Figure 1).

We studied the effect of adaptation by using prolonged presentation times (150 s) for the adapting stimulus that was subsequently followed by a brief blank period and a test stimulus. We compared responses to the following conditions: (1) identical random pattern, where the test stimulus was identical to the adapting stimulus, (2) different random pattern, where the test stimulus was a different random pattern from the adapting stimulus, and (3) random-to-collinear pattern, where the adapting stimulus was a random pattern while the test stimulus was a collinear pattern. The average rotation change of the line segments used for the stimulus generation in the different random pattern and the random-to-collinear pattern condition was the same. Thus, stronger rebound effects for conditions with collinear than random patterns would indicate visual areas responsive to global visual configurations.

Localization of ROIs

For each individual subject, we localized the visual areas (ROIs: V1, V2/V3, V4) based on both functional and anatomical criteria (Gattass et al., 1981, 1988; Desimone and Ungerleider, 1986; Brewer et al., 2002). Specifically, area V1 was estimated to cover most of the operculum extending laterally up to about 1 mm posterior to the Lunate sulcus and medially within the calcarine sulcus, area V2/V3 was within the lunate and inferior occipital sulcus, and area V4 was dorsally on the prelunate gyrus between the lunate and superior temporal sulcus and ventrally in the anterior bank of inferior occipital sulcus. The voxels within these anatomically selected areas that responded significantly more strongly ($p < 0.0032$, corrected) to a full field rotating polar stimulus than to blank background stimulation were identified as the regions of interest (ROI) for the analysis of the responses in the adaptation experiment (Figure 2). These ROIs correspond most largely to the ones revealed by retinotopic mapping in recent monkey fMRI studies (Brewer et al., 2002).

Here we report responses during the adaptation experiment for areas V1 and V2/V3 where the activation was more robust. The weaker activation observed in area V4 was possibly due to the properties of the stimulus used for the adaptation experiment (statically flashed stimulus) that may not activate strongly these areas in the anesthetized monkey.

Adaptation and Rebound Effects

For each subject, we computed the time course of the normalized fMRI response from the initial 30 s background stimulation period by averaging the data from all the voxels within each one of the independently defined ROIs for each condition. Details on the analysis of the data are reported in previous studies (Tolias et al., 2001). Briefly, we calculated the initial and the rebound responses of the time course. The initial response was defined as the peak response (10 s) of the filtered activity (digital eighth order [48 dB/oct] low pass Butterworth filter with cutoff frequency of 0.125 Hz) after the onset of the adapting stimulus. The rebound response was defined as the peak response of the filtered activity after the onset of the test stimulus. We also calculated an adaptation response as the mean response before the onset of the test stimulus.

As shown in Figures 3A and 3B, responses in V1 showed the basic adaptation effect; that is, strong responses to the onset of the adapting stimulus decreased with prolonged presentation of the stimulus. A rebound of activity was observed for orientation changes in the test stimulus. That is, when the test stimulus was different from the adapting stimulus, increased fMRI responses were observed, compared to the low fMRI responses when the test stimulus was identical to the adapting stimulus. More importantly, we observed a stronger rebound effect for collinear than for random patterns, suggesting selective responses to global shapes. In particular, a repeated measures ANOVA with condition (identical random pattern, different random pattern, and random-to-collinear pattern) and time (initial, adap-

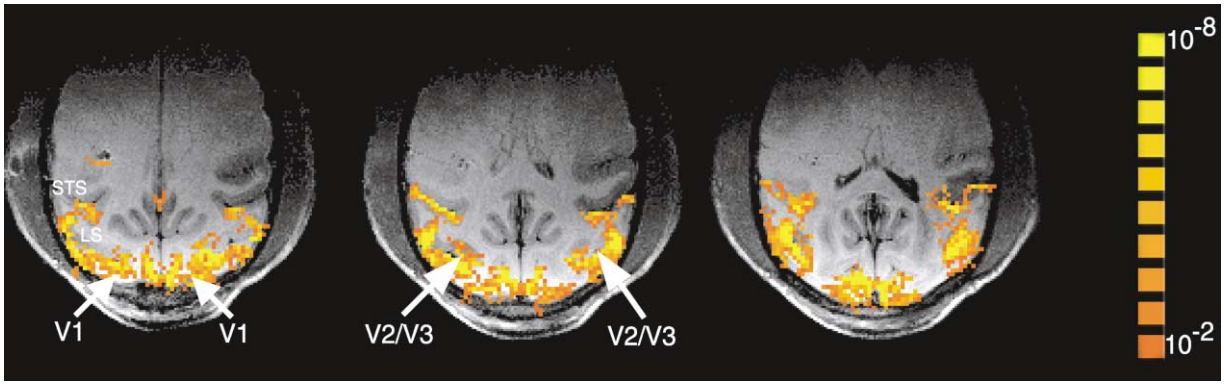

Figure 2. Localization of the Visual Areas in the Monkey Brain

Three consecutive slices (posterior to anterior) from one subject showing the visual areas (V1, V2/V3) that were selected as regions of interest for the analysis of the adaptation experiment. These regions responded significantly more strongly to polar rotating rings than to blank stimulation periods. Significance charts indicate the results of t tests. The arrows point to the activated visual areas, the borders of which were identified based on anatomical criteria (Desimone and Ungerleider, 1986; Gattass et al., 1981, 1988). Major sulci are labeled: LS, lunate sulcus; STS, superior temporal sulcus.

tation, rebound response) as factors showed main effects of condition [$F(2,36) = 18.8$, $p < 0.001$] and time [$F(2,36) = 42.6$, $p < 0.001$] and an interaction effect [$F(4,36) = 27.8$, $p < 0.001$]. Contrast analysis showed rebound of activity when the test stimulus was a different random pattern from the adapting stimulus or a collinear pattern but not when it was identical to the adapting stimulus. That is, significantly stronger rebound than adaptation responses were observed for the different random pattern [$F(1,36) = 68.7$, $p < 0.001$] and the random-to-collinear pattern [$F(1,36) = 262.4$, $p < 0.001$] conditions. However, no significant difference was observed between the rebound and the adaptation responses for the identical random pattern condition [$F(1,36) = 3.5$, $p = 0.1$]. Finally, we observed a significantly stronger rebound effect for the random-to-collinear pattern than the different random pattern condition [$F(1,36) = 35.6$, $p < 0.001$], suggesting responses selective to collinear patterns.

Thus, these results showed selectivity in V1 for orientation but more importantly for collinear contours. Specifically, we observed fMRI rebound of activity for changes in the orientation of the local elements in the test stimulus. This effect is consistent with neurophysiological evidence for orientation selectivity in these regions revealed by adaptation (e.g., Movshon and Lennie, 1979; Carandini et al., 1997; Mueller et al., 1999; Dragoi et al., 2000). More importantly, we observed a stronger rebound effect when the orientation change in the test stimulus resulted in a collinear than a random pattern. This effect indicates that neural populations in V1 enhanced selectively their responses in the presence of "good continuation" (Kofka, 1935) induced by line segment collinearity. These findings are consistent with previous neurophysiological studies (Kapadia et al., 1995, 1999; Zipser et al., 1996; Lamme et al., 1998; Polat et al., 1998) suggesting that neural populations in V1 are involved in the processing of global rather than simply local stimulus features.

As shown in Figures 3C and 3D, the basic adaptation and rebound effects for orientation changes in the test stimulus were observed also in area V2/V3. In particular, a repeated measures ANOVA showed main effects of condition [$F(2,36) = 45.7$, $p < 0.001$] and time [$F(2,36) = 142.8$, $p < 0.001$] and an interaction between condition and time [$F(4,36) = 24.2$, $p < 0.001$]. Contrast analysis showed adaptation over time; that is, there is significantly stronger responses for the initial than for the adaptation responses [$F(1,36) = 283.2$, $p < 0.001$]. Moreover, we observed significantly stronger rebound than adaptation responses for the different random pattern [$F(1,36) = 93.6$, $p < 0.001$] and the random-to-collinear [$F(1,36) = 178.4$, $p < 0.001$] conditions, but no significant difference for the identical random pattern condition [$F(1,36) = 4.9$, $p = 0.06$].

Surprisingly, in contrast to responses in V1, we did not observe selective rebound responses to collinear patterns in V2/V3. A small effect was observed in the reverse direction; that is, the rebound effect for the different random pattern condition was significantly stronger than for the random-to-collinear pattern condition [$F(1,36) = 8.4$, $p < 0.05$]. A possible explanation is that the larger RFs in V2/V3 compared to V1 (Gattass et al., 1981, 1988) are stimulated not only by collinear elements but also by randomly oriented background elements. Thus, the lower signal (collinear elements)-to-noise (background randomly oriented elements) ratio in the RF of neurons in V2/V3 may result in lower selectivity for collinear contours. It is possible that this effect is due to suppressive modulation of the activation for collinear contours by the surrounding elements. This hypothesis is consistent with previous findings showing that masking of the target by background elements may result in suppressive effects (Blakemore and Tobin, 1972; Knierim and van Essen, 1992; DeAngelis et al., 1994; Grinvald et al., 1994; Kastner et al., 1997; Sengpiel et al., 1997; Li et al., 2000; Nothdurft et al., 2000; Polat and Bonneh, 2000). Further analysis in central and peripheral subregions of V1 and V2 that differ in their RF size addressed this possibility.

Responses in Central and Peripheral Subregions

To investigate the local integration processes in V1 and V2 subregions with different RF size, we compared fMRI

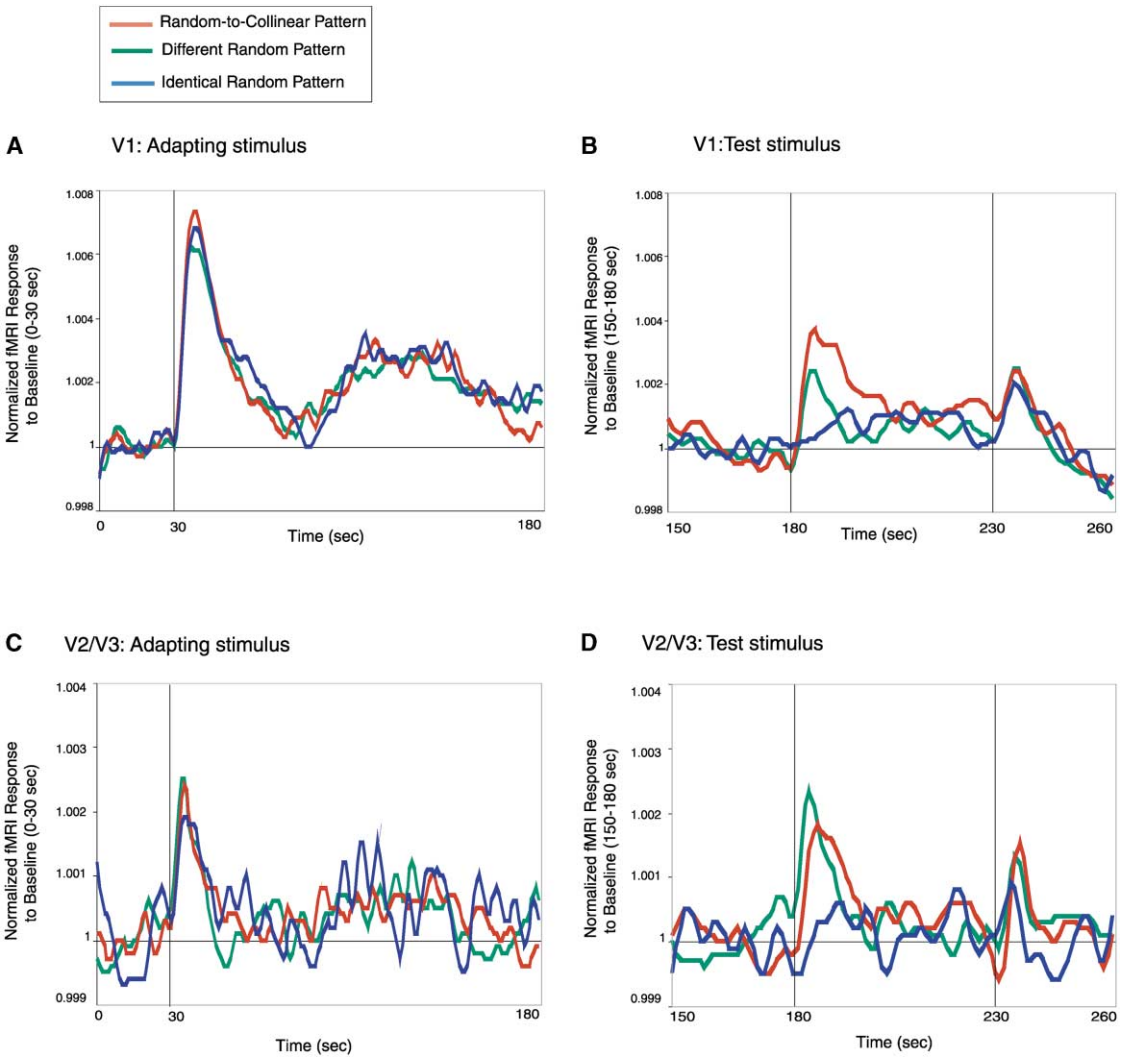

Figure 3. fMRI Responses: Monkey fMRI Study

Normalized fMRI responses (averaged across trials and subjects for all voxels in each ROI) reported in V1 (A and B) and V2/V3 (C and D) for each one of the experimental conditions: random-to-collinear pattern (red), different random pattern (green), and identical random pattern (blue). Plots (A) and (C) show fMRI responses to the onset of the adapting stimulus (30 s) and the adaptation effect; that is, decreased responses during the stimulus presentation (up to 180 s). The baseline for the plotted normalized fMRI response was the initial 30 s background stimulation period before the stimulus onset. The colors of the curves are of no importance in these plots because the adapting stimulus was always the same random pattern across conditions. The oscillations observed during the adaptation period may be due to stimulus flickering. Plots (B) and (D) show fMRI responses to the test stimulus normalized to a 30 s period before the test stimulus onset. Specifically, the rebound of activity is plotted for the random-to-collinear pattern and different random pattern conditions compared to the adapted responses to the identical random pattern condition. The test stimulus was presented from 180 s until 230 s and was followed by a blank stimulus as indicated by the off response (230 s).

responses in central (up to 6°) and peripheral V1 and V2 (Gattass et al., 1981, 1988; Burkhalter and van Essen, 1986; Felleman and van Essen, 1987). Central V1 was defined on the surface of the posterior visual cortex from the foveal representation laterally on the operculum to the midline, while peripheral V1 was defined within the calcarine sulcus. We considered central V2 to lie 2 mm on the cortical surface posterior to the lunate sulcus and extend 2 mm within the posterior bank of the lunate sulcus, while peripheral V2 was located further into the posterior bank of the lunate sulcus excluding the fundus. The localization of the central and peripheral V1 was possible in all monkeys tested in this study. The localization of the central and peripheral V2 on the slice selection for this study was possible only in three monkeys.

To compare across regions, we calculated an adaptation index by dividing the rebound response to each condition by the rebound response to the identical random pattern condition (Figure 4A). A ratio of 1 indicates adaptation, while significantly higher responses than 1 indicate rebound of activity. We observed selectivity for collinear contours (i.e., stronger rebound for collinear than random patterns) in peripheral V1 and central V2, but not in central V1 or peripheral V2. Specifically, a repeated measures ANOVA showed main effects of ROI (central V1, peripheral V1, central V2, peripheral V2)

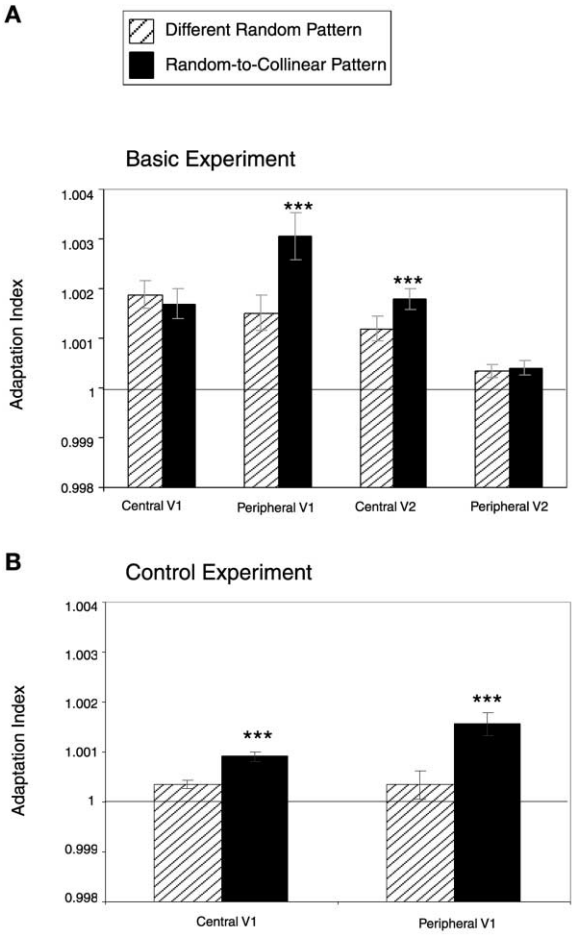

Figure 4. fMRI Adaptation Index across Visual Areas in the Monkey Brain

An fMRI adaptation index (fMRI responses in each condition/fMRI responses in the identical random pattern condition) reported for (A) the basic fMRI study and (B) a control experiment where the size of the stimulus patterns was half of the size of the patterns used in the basic experiment. A ratio of 1 (horizontal line) indicates adaptation. This adaptation index is plotted for the responses to the random-to-collinear pattern (solid bars) and to the different random pattern (striped bars) conditions across visual areas. The error bars indicate standard errors on the percent signal change averaged across scans and subjects. Significant differences are indicated by three asterisks ($p < 0.001$).

[$F(3,54) = 23.48$, $p < 0.001$] and condition [$F(2,54) = 46.30$, $p < 0.001$] as well as an interaction effect [$F(6,54) = 24.96$, $p < 0.001$]. Significantly higher rebound than 1 was observed across the tested visual areas when the test stimulus was a collinear pattern or a random pattern different than the adapting stimulus [$F(1,54) = 563.05$, $p < 0.001$]. However, significantly stronger rebound for collinear than random patterns was observed in peripheral V1 [$F(1,54) = 73.78$, $p < 0.001$] and central V2 [$F(1,54) = 11.82$, $p < 0.001$], but not in the central V1 [$F(1,54) = 1.2$, $p = 0.29$] or peripheral V2 [$F(1,54) < 1$, $p = 0.41$].

A possible explanation of these results is that the contribution of the early visual areas in the analysis of global contours may depend on signal-to-noise ratio within the RFs of neurons that vary in their size across areas (Gattass et al., 1981, 1988). That is, the lack of selectivity to collinear patterns in central V1 could be due to the low signal-to-noise ratio in the small RFs of neurons (0.25° or smaller for most neurons). This ratio is increased in peripheral V1 and central V2 where neurons have larger RF size than central V1 (i.e., the range for the RF size in peripheral V1 is 1.5°–2° and in central V2 is 0.05°–2.5°), and as a result enhanced responses to collinear patterns are observed (Kapadia et al., 1995, 1999; Zipser et al., 1996; Lamme et al., 1998; Polat et al., 1998). However, neural populations in peripheral V2 with increased RF size (i.e., within a range of 2.5°–4°) are stimulated not only by collinear but also by many randomly oriented background elements. As a result, it is possible that the signal-to-noise ratio in this region is decreased and reduced selectivity to collinear patterns is observed.

Supporting evidence for the possible role of RF size in this integration process comes from a control experiment that followed similar design as the adaptation experiment but used stimuli half the size of the original ones. The results showed responses selective to collinear patterns not only in peripheral but also in central V1 when the size of the elements was reduced. As shown in Figure 4B, we observed significantly stronger rebound responses for the different random pattern and the random-to-collinear pattern conditions than the identical random pattern condition in both central [$F(1,18) = 16.5$, $p < 0.001$] and peripheral [$F(1,18) = 18.7$, $p < 0.001$] V1. More interestingly, we observed a significantly stronger rebound effect for the random-to-collinear pattern than the different random pattern condition in both central [$F(1,18) = 447.5$, $p < 0.001$] and peripheral [$F(1,18) = 16.1$, $p < 0.001$] V1. Thus, change in the stimulus scale that increased the number of collinear elements in the RFs of central V1 neurons resulted in selective responses to collinear patterns in this region.

Human fMRI Studies

In a similar fashion to the monkey fMRI studies, we tested for responses to collinear versus random patterns in human subjects. Our goals were 2-fold: (1) to investigate the integration process across primate species using the same fMRI technique and similar paradigms, and (2) to test for responses in higher visual areas that are more easily activated within single subject sessions in the awake human than in the anesthetized monkey.

The random patterns consisted of a square area filled with randomly oriented elements, while the collinear patterns consisted of two concentric closed contours of collinear elements that were embedded in a field of randomly oriented elements (Figure 5). The stimuli were rendered with Gabors; that is, oriented elements similar to line segments that are defined by sinusoidal luminance features with Gaussian envelopes that model roughly the RF structure of V1 simple cells.

An event-related adaptation paradigm (Kourtzi and Kanwisher, 2000, 2001) was used to study the effect of adaptation to fast sequential presentation of two stimuli (same or different) in a trial. We compared responses to the following conditions: (1) identical random pattern, where the same random pattern was presented twice

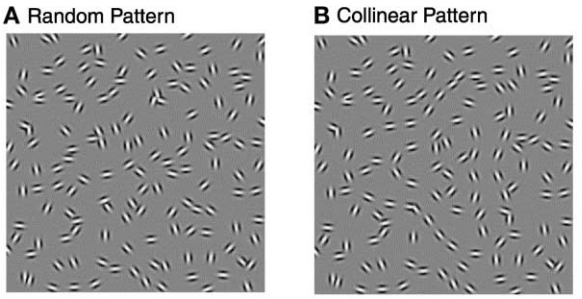

Figure 5. Stimuli for the Human fMRI Adaptation Study

Examples of (A) the random patterns and (B) the collinear patterns used as stimuli.

in a trial, (2) different random pattern, where two different random patterns were presented in a trial, (3) random-to-collinear pattern, where the first stimulus in a trial was a random pattern while the second stimulus was a collinear pattern. Similarly to the monkey fMRI studies, stronger rebound effects for collinear than for random patterns would indicate visual areas responsive to global visual configurations.

Localization of ROIs

Early visual areas were identified individually for each subject as regions of interest (ROIs) using standard retinotopic mapping techniques (Engel et al., 1994; Sereno et al., 1995; DeYoe et al., 1996). An additional ROI comprising the lateral occipital complex (LOC) was identified individually for each subject as the set of contiguous voxels in the ventral occipitotemporal cortex that were activated more strongly ($p < 10^{-4}$, corrected) by intact than by scrambled images of objects presented in two localizer scans (Figure 6). This region has been suggested to be involved in the analysis of visual shape (Malach et al., 1995; Kanwisher et al., 1996) and object recognition (Grill-Spector et al., 2000; Bar et al., 2001). The magnitude of the response in these ROIs was then measured for each subject in each condition of the event-related adaptation experiment.

Adaptation and Rebound Effects

For each subject, we computed the average time course of the percent signal change from the fixation baseline in each ROI for each experimental condition as described previously (Kourtzi and Kanwisher, 2000, 2001). Consistent with prior reports (Boynton et al., 1996; Cohen, 1997; Dale and Buckner, 1997) on the hemodynamic response lag of the fMRI response, the peak response (i.e., the average of the percent signal change at 5 and 6 s after trial onset) was taken as the measure of the response magnitude.

Responses in Early Retinotopic Regions

As shown in Figure 7A, we observed that early visual areas in the humans (just as in the monkeys) encode orientation changes in random and collinear patterns. Specifically, a repeated measures ANOVA on the peak responses for the retinotopic regions showed a significant effect of condition (identical random pattern, different random pattern, and random-to-collinear pattern) in V1 [$F(2,22) = 8.39$, $p < 0.01$], V2 [$F(2,22) = 4.30$, $p < 0.05$], V3a [$F(2,30) = 5.40$, $p < 0.01$], and V4v [$F(2,22) = 4.34$, $p < 0.01$] but not in V3 [$F(2,22) < 1$, $p = 0.49$] and Vp [$F(2,22) < 1$, $p = 0.48$].

Further contrast analysis in areas V1, V2, V3a, and V4v showed a significant rebound effect for both random and collinear patterns; that is, the responses to the different random pattern and random-to-collinear pattern conditions were significantly stronger than the responses to the identical random pattern condition [V1 $F(1,22) = 15.56$, $p < 0.001$; V2 $F(1,22) = 8.25$, $p < 0.01$; V3a $F(1,22) = 10.68$, $p < 0.01$; V4v $F(1,22) = 6.43$, $p = 0.01$]. Surprisingly, the rebound effect in these regions was not different for collinear and random patterns. Specifically, the responses to the random-to-collinear pattern condition were not significantly different than the responses to the different random pattern condition [V1 $F(1,22) = 1.2$, $p = 0.28$; V2 $F(1,22) < 1$, $p = 0.55$; V3a $F(1,22) < 1$, $p = 0.72$; V4v $F(1,22) = 2.25$, $p = 0.14$].

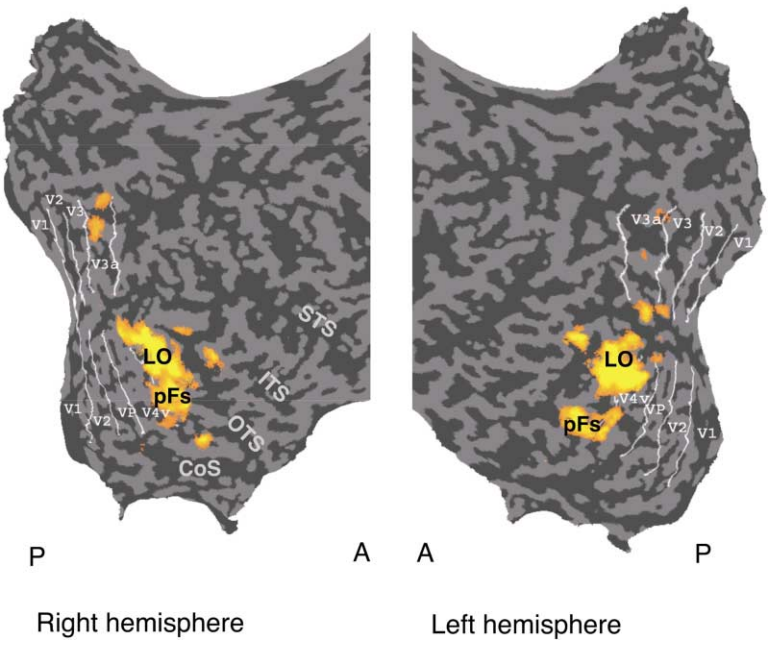

Figure 6. Localization of the Visual Areas in the Human Brain

Functional activation maps for one subject showing the early retinotopic regions and the LOC. The functional activations are superimposed on flattened cortical surfaces of the right and left hemispheres. The sulci are coded in darker gray than the gyri and the anterior-posterior orientation is noted by A and P. Major sulci are labeled: STS, superior temporal sulcus; ITS, inferior temporal sulcus; OTS, occipitotemporal sulcus; CoS, collateral sulcus. The borders (shown by lines) of the early visual regions (V1, V2, VP, V3, V3a, V4v) were defined with standard retinotopic techniques. The LOC was defined as the set of all contiguous voxels in the ventral occipitotemporal cortex that were activated more strongly ($p < 10^{-4}$) by intact than by scrambled images of objects. The posterior (LO) and anterior (pFs) regions of the LOC were identified based on anatomical criteria.

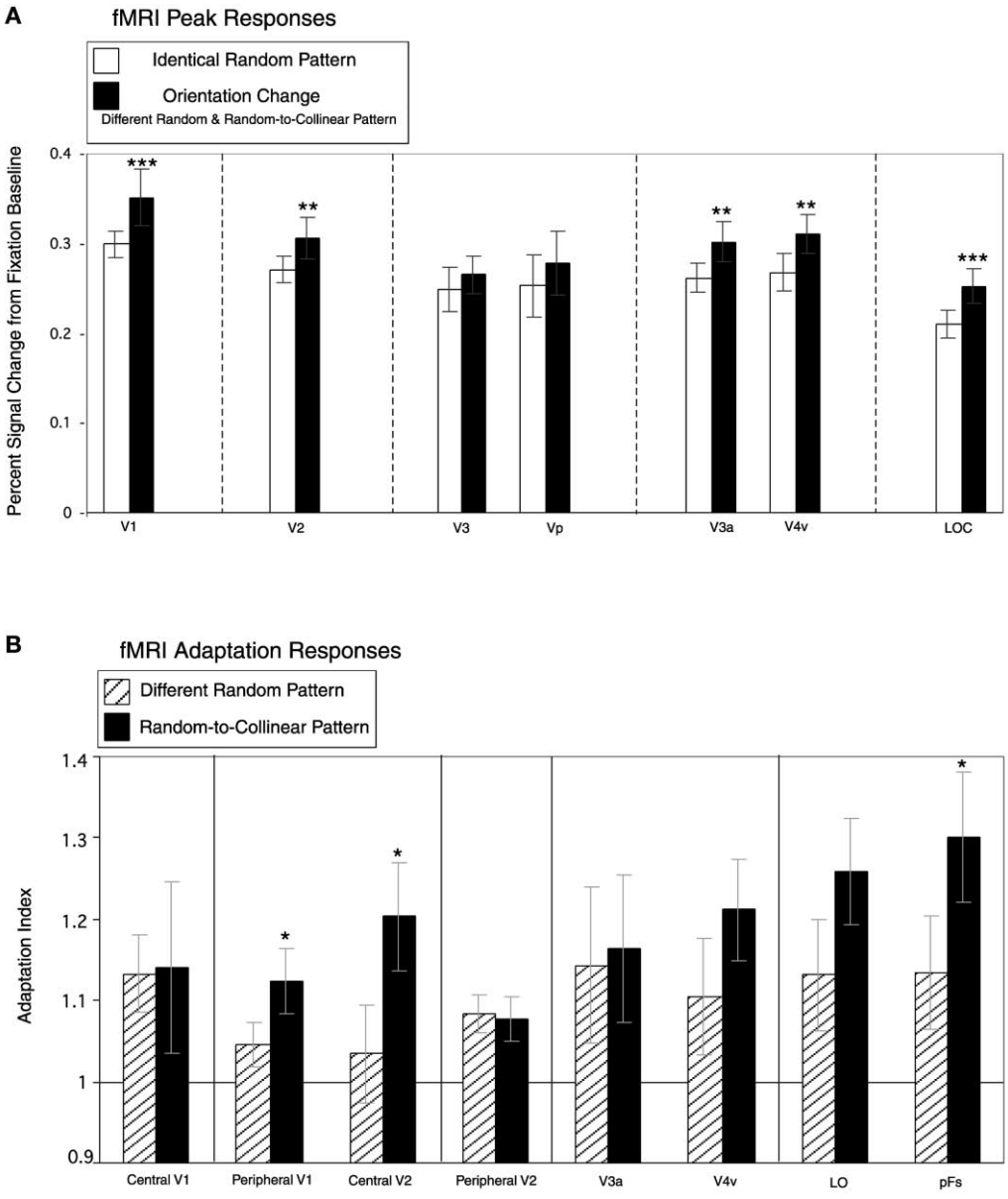

Figure 7. fMRI Responses: Human fMRI Study

(A) fMRI peak responses. Average fMRI percent signal increases (from the fixation baseline trials) at the peak time points (5–6 s after the trial onset) of the event-related responses. Responses are plotted for the identical random pattern condition (solid white bars) where no change occurred in the test stimulus compared to orientation changes (solid black bars) in the test stimulus (different random pattern and random-to-collinear pattern condition). The fMRI responses are shown for early (V1, V2, V3, Vp, V3a, V4v) and higher (LOC) visual areas. The areas are grouped by separating dotted lines based on their RF size (Felleman and van Essen, 1987; Smith et al., 2001). The error bars indicate standard errors on the percent signal change averaged across scans and subjects. Significant differences are indicated by asterisks (two asterisks for $p < 0.01$, three for $p < 0.001$).

(B) fMRI adaptation index. An fMRI adaptation index (percent signal change in each condition/percent signal change in the identical random pattern condition) reported for the random-to-collinear pattern (solid black bars) and the different random pattern (striped bars) conditions across visual areas. A ratio of 1 (horizontal line) indicates adaptation. This adaptation ratio is shown for central and peripheral subregions of V1 and V2, V3a, V4v, posterior (LO) and anterior (pFs) subregions of the LOC. The areas are grouped by separating doted lines based on their RF size (Felleman and van Essen, 1987; Smith et al., 2001). The error bars indicate standard errors on the percent signal change averaged across scans and subjects. Significant differences are indicated by one asterisk ($p < 0.05$).

Responses in Central and Peripheral Subregions

Analysis of the responses in central and peripheral subregions of V1 showed that the rebound effect was significantly stronger for collinear than for random patterns in peripheral [$F(1,22) = 5.89$, $p < 0.05$] but not in central [$F(1,22) < 1$, $p = 0.91$] V1. Surprisingly, similar analysis in V2 showed that the rebound effect was significantly stronger for collinear than for random patterns in central [$F(1,22) = 7.86$, $p < 0.01$] but not in peripheral [$F(1,22) < 1$, $p = 0.82$] V2.

These findings are consistent with the patterns of results observed in the monkey fMRI study. As discussed

previously, a possible interpretation of these results is that selective responses to collinear contours in early visual areas may be determined by the signal-to-noise ratio within the neuronal RFs that differ in their size (Smith et al., 2001) within and across these regions.

Responses in Higher Visual Areas

Analysis of the responses in the LOC showed selective responses to collinear contours. Specifically, a repeated measures ANOVA in the LOC showed a significant [$F(2,30) = 9.61$, $p < 0.001$] effect of condition (identical random pattern, different random pattern, and random-to-collinear pattern). Furthermore, contrast analysis showed a significant rebound effect for both random and collinear patterns. That is, the responses to the different random pattern and the random-to-collinear pattern conditions were significantly stronger than the responses to the identical random pattern condition [$F(1,30) = 13.58$, $p < 0.001$]. More interestingly, the rebound effect for collinear patterns was significantly stronger than for random patterns; that is, the responses to the random-to-collinear pattern condition were significantly stronger than the responses to the different random pattern condition [$F(1,30) = 5.63$, $p < 0.05$]. This effect was observed primarily in the anterior regions of the LOC (posterior fusiform [pFs]) [$F(1,30) = 6.77$, $p = 0.01$] and rather marginally in the posterior regions (lateral occipital [LO]) [$F(1,30) = 4.04$, $p = 0.05$].

This selectivity for collinear contours in the LOC cannot be accounted by the amount of signal-to-noise ratio within the neuronal RF because the large RFs in this region are stimulated by the whole stimulus where the number of collinear elements is smaller than that of the background elements. It is possible that responses in this area are modulated more strongly by combinations of features rather than by single elements. These results are consistent with previous imaging studies, suggesting that the LOC is involved in the processing of the perceived global shape. Interestingly, anterior subregions of the LOC have been suggested to process complete objects rather than their fragments that are thought to be represented in posterior subregions (Grill-Spector et al., 1998b; Lerner et al., 2001, 2002).

Comparison across Visual Areas

To further compare responses across areas, we calculated an adaptation index by dividing the rebound response to each condition by the rebound response to the identical random pattern condition. As shown in Figure 7B, a ratio of 1 indicates adaptation, while significantly higher responses than 1 indicate recovery from adaptation. A stronger adaptation index for collinear than random patterns indicates areas that respond selectively to collinear patterns. This analysis was conducted on regions (V1, V2, V3a, V4v, LOC) that showed significant rebound effect (Figure 7A).

We observed selectivity for collinear patterns in peripheral V1, central V2, and the anterior subregion of the LOC (pFs). In particular, significantly stronger rebound for collinear than for random patterns was observed in peripheral V1 [$F(1,22) = 5.79$, $p < 0.05$], central V2 [$F(1,22) = 4.14$, $p = 0.05$], and pFs [$F(1,22) = 4.30$, $p < 0.05$], but not in central V1 [$F(1,22) < 1$, $p = 0.43$], peripheral V2 [$F(1,22) < 1$, $p = 0.93$], V3a [$F(1,22) = 3.49$, $p = 0.09$], V4v [$F(1,22) < 1$, $p = 0.37$], or LO [$F(1,22) = 1.64$, $p = 0.20$]. The magnitude of selectivity for collinear patterns was similar across peripheral V1, central V2, and the anterior subregions of the LOC (pFs). Specifically, a repeated ANOVA on the adaptation index across conditions showed significantly stronger rebound effect for the collinear than for the random patterns [$F(1,22) = 10.39$, $p < 0.01$] but no significant difference [$F(1,22) < 1$, $p = 0.42$] across areas (peripheral V1, central V2, pFs).

Discussion

Traditionally, early visual areas have been implicated in the analysis of local features (e.g., orientation), while higher visual areas have been implicated in the processing of shapes. The goal of our study was to quantify the involvement of the different visual areas in the human and nonhuman primate brain in the processing of global shapes. An important aspect of shape processing is sensitivity to "good continuation" (Kofka, 1935) induced by the collinearity of local elements. Thus, we chose to investigate shape processing across visual areas by testing for selectivity to collinear contours with similar fMRI adaptation paradigms in both monkeys and humans.

Our findings demonstrate that not only higher but also early visual areas are involved in the analysis of global shape, to the extent that the sensitivity of small neural populations that process local image attributes is strongly affected by the global properties of the image. In particular, we observed stronger recovery from adaptation when orientation changes in the adapting stimulus resulted in a collinear rather than a different random pattern that shared the same average orientation change. It is possible that the observed selectivity to collinear patterns after adaptation reflects overall higher sensitivity to collinear than to random patterns and it could have been detected with conventional fMRI techniques. In this study, we chose fMRI adaptation as a more sensitive tool to detect selectivity to collinearity across visual areas. Our findings are consistent with previous neurophysiological studies showing that early visual areas (e.g., V1, V2) may respond to global rather than simple local features (Gilbert, 1992, 1998; Allman et al., 1985; Lamme et al., 1998; Fitzpatrick, 2000, for reviews).

Moreover, our studies provide novel evidence that the integration of local elements to global shapes may depend on the RF size of the neurons within and across early visual areas. In particular, the signal (collinear elements)-to-noise (background randomly oriented elements) ratio within the neuronal RFs that vary in their size across areas appeared to modulate the fMRI selectivity to collinear patterns in early visual areas. Thus, our findings suggest that the unified perception of global shapes involves multiple visual areas that may process collinearity at different spatial scales. Future studies are needed to test further the sensitivity to collinear lines versus global shapes and the selectivity to different global shapes across visual areas.

Comparison across Species

One of the main goals of our study was to investigate the integration of local elements to global shapes in both the monkey and the human brain. To this end, we

used the same fMRI technique in an attempt to bridge the gap between previous monkey electrophysiological and human fMRI findings on the neural processing of shapes.

However, it is important to note the differences between the monkey and the human fMRI experiments in our study. First, the monkey subjects were anesthetized, whereas the human subjects were awake. As a result, differential attention or eye movements across conditions could modulate the fMRI responses in the human compared to the monkey studies. Second, the stimuli used in the monkey experiments consisted of line segments while the stimuli in the human experiments consisted of Gabors. The advantage of Gabor elements compared to line segments is that due to their Gaussian properties they are thought to stimulate neurons tuned to their orientation but not to orthogonal edges. Finally, a prolonged fMRI adaptation design was used for the monkey studies while a rapid fMRI adaptation design was used in the human studies. Several neurophysiological studies have reported adaptation effects for rapid stimulus presentations (Mueller et al., 1999; Lisberger and Movshon, 1999) and stimulus repetition (Miller et al., 1991, 1996) similar to adaptation effects observed after prolonged stimulus presentation. The main advantage of using a rapid event-related adaptation paradigm (Dale and Buckner, 1997; Rosen et al., 1998) for awake human fMRI studies is that it allows the collection of fMRI data across large numbers of trials in the limited time that the subjects can remain attentive and still in the scanner and facilitates the simultaneous collection of psychophysical data.

The similarity of the findings across species, despite these differences between the monkey and the human fMRI studies, provides strong evidence that similar mechanisms mediate the integration of local elements to global shapes in the human and nonhuman primate brain. To control for the possible effect of eye movements in the human studies, we trained the subjects to fixate and monitored the eye position for three subjects at a sampling rate of 1000 Hz by an infrared eyetracking system in the scanner (Cambridge Research). No significant differences [$F(3,6) = 1.022$, $p = 0.4465$] were observed in the mean eye position across conditions (fixation, 0.064°; identical random pattern, 0.103°; different random pattern, −0.153°; random-to-collinear, −0.038°), indicating that the subjects maintained fixation equally well across all conditions. Thus, the stronger rebound of activity for collinear than random patterns observed in our human experiments is unlikely to be due to differences in the eye movements across conditions.

Furthermore, analysis of the subjects' behavioral data indicates that our fMRI findings could not be due to differential attention of the subjects across conditions. In particular, the subjects' performance indicates that the different random pattern condition (32% correct responses, 655 ms reaction time from onset of second stimulus in a trial) was more difficult than the identical random pattern (80% correct, 517 ms) and the random-to-collinear pattern (72% correct, 593 ms) conditions. That is, stronger rebound responses observed for collinear (random-to-collinear pattern) than random patterns (different random pattern) could not be accounted by higher difficulty or attentional demands of the task performed in the first compared to the later condition.

Finally, to further control for the methodological differences between studies, we conducted an additional human fMRI experiment on three subjects using similar stimuli (line segment patterns) and paradigm (prolonged adaptation) to the ones used for the monkey experiments. The subjects performed a dimming task; that is, they were instructed to indicate luminance changes on the fixation point. The high performance of the subjects in this task across all conditions ensured that they were fixating and that they were equally attentive across conditions. The results in the early and higher visual areas showed similar adaptation and stronger rebound effects for collinear than for random patterns as in our previous monkey and human fMRI experiments. These findings suggest that the collinearity effect that was observed across all experiments could not be due to differences in the subject's attention or the experimental paradigms. Thus, these findings provide evidence for common mechanisms in the human and nonhuman primate brain that are involved in the processing of global contours.

Recurrent Mechanisms of Global Shape Processing

What are the neural mechanisms that mediate the integration of local elements to global shapes? It has been proposed that this integration process is mediated by lateral connections that mediate visual processing in the surround of the classical RF center of V1 neurons (Allman et al., 1985; Fitzpatrick, 2000, for reviews). As a result, stimuli in the surround of the RF may cause contextual facilitative or suppressive effects on the response to stimuli in the classical RF (Hubel and Wiesel, 1965; Maffei and Fiorentini, 1976). While long-range connections have been suggested to link neurons of similar orientation tuning and mediate contour integration (Gilbert and Wiesel, 1989; Gilbert, 1992, 1998; Malach et al., 1993; Bosking et al., 1997), short-range connections are thought to link neurons with different orientation preferences and mediate detection of border discontinuities (Das and Gilbert, 1997, 1999). Recent studies have proposed that contextual effects may be also mediated by feedback from higher areas (e.g., Salin and Bullier, 1995; Zipser et al., 1996; Lamme et al., 1999; Lamme and Roelfsema, 2000; Li et al., 2000; Mareschal et al., 2001).

This recurrent processing of visual information via local connections and feedback interactions could account for our findings. Specifically, the perception of collinear contours requires both integration of the similarly oriented target elements and segmentation from their cluttered background. The increased selectivity for collinear patterns in peripheral compared to central V1 suggests a local process of linking similarly oriented elements together. However, the decreased selectivity in peripheral compared to central V2 suggests suppressive processes from distractor elements in the background. That is, responses to collinear patterns in V1 neurons with small RFs may reflect integration of a small number of collinear elements in local neighborhoods. Larger RFs in peripheral V2 may pool together a larger number of elements from both the target shape

and the background. At this stage, global processes, namely figure-ground segmentation (Lamme 1995; Zipser et al., 1996; Lee et al., 1998; Rossi et al., 2001) and figure border assignment (Bakin et al., 2000; Zhou et al., 2000), mediate the segmentation of the target and facilitate the successful integration of the collinear elements. These processes implicate primarily V2 neurons and are mediated by suppressive effects between target and distractor elements (Fitzpatrick, 2000, for review). Their output influences responses of V1 neurons via feedback connections as shown by stronger responses to figures than the background at later latencies (Zipser et al., 1996; Lamme et al., 1999). After figure-ground segmentation has been achieved, higher visual areas (e.g., LOC) encode selectively the global shapes and their responses could influence responses in early visual areas via feedback mechanisms.

Interestingly, these recurrent processing mechanisms have been suggested to operate in the surround of the classical RF center of neurons even for stimuli distant from the borders of the RF boundaries (e.g., Lamme 1995; Zipser et al., 1996). However, our findings showed that selectivity to collinear contours was modulated in early visual areas by the signal-to-noise ratio within the range of the classical RF size known for each area (Gattass et al., 1981, 1988; Smith et al., 2001). These results suggest that integration processes can be explained by spatial summation mechanisms within or close to the RF borders of neurons (e.g., DeAngelis et al., 1992; Sceniak et al., 1999; Rossi et al., 2001; Smith et al., 2002). Further studies are required to test the effect of stimulus density and size on the selectivity for global shapes across visual areas.

Conclusions

In conclusion, our findings suggest that unified shape perception involves multiple visual areas that may integrate local elements to global shapes at different spatial scales. Contour integration is only one of the phenomena characterizing coherent visual perception that could be attributed to distributed processing of global shape information. Others include the perception of illusory contours (von der Heydt and Peterhans, 1989; Peterhans and von der Heydt, 1989; Mendola et al., 1999; Lee and Nguyen, 2001), detection of curvature (Dobbins et al., 1987), pop-out of targets (Knierim and van Essen, 1992; Polat and Sagi, 1993; 1994; Zenger and Sagi, 1996; Kastner et al., 1997; Polat, 1999; Nothdurft et al., 1999; Li et al., 2000), and perception of surfaces (Paradiso and Nakayama, 1991; Nakayama and Shimojo, 1992; Moller and Hurlbert, 1996; Rossi et al., 1996; MacEvoy et al., 1998).

The present study advances our understanding of these perceptual phenomena that constitute key puzzles for object recognition in several important respects. First, although previous studies have provided evidence for global processing in early visual areas (e.g., Knierim and van Essen, 1992; Kapadia et al., 1995; Lamme, 1995; Zipser et al., 1996; Polat et al., 1998), they have used rather simple stimuli (e.g., single oriented lines or textured targets) compared to the complex objects used by a different set of studies that suggest higher visual areas as the main locus of shape processing (e.g., Gross et al., 1972; Logothetis and Sheinberg, 1996; Tanaka, 1996; Grill-Spector and Malach, 2001; Haxby et al., 2001). Our study used the same stimuli (i.e., global shapes consisting of local oriented elements) to investigate the processing of both local and global features across cortical areas. Second, the use of fMRI has allowed us to test for responses across all visual areas simultaneously in the same subjects and with the same stimuli and experimental paradigms. Finally, by using fMRI, our study bridges the gap between previous monkey electrophysiological and human fMRI findings on the neural processing of shapes. The similarity of the findings across species provides novel evidence for similar neural mechanisms underlying unified visual perception in the human and nonhuman primate brain. Future studies comparing electrophysiological and fMRI responses in alert behaving monkeys and imaging in humans are required for testing the neural mechanisms and the generality of the principles underlying visual perception across species. These studies will provide further insights in the functional spatial and temporal connectivity across visual areas that contribute to visual awareness in the primate brain.

Experimental Procedures

Monkey fMRI Studies

Subjects

Experiments were conducted in five monkeys (*Macaca mulatta*) weighing 5.5 to 7 kg. All procedures for the fMRI imaging and stimulus presentation were described previously (Logothetis et al., 1999).

Stimuli

To localize visual areas as regions of interest (ROI), we used a 100% contrast full field rotating checkerboard polar pattern stimulus (30° horizontal × 23° vertical). The spatial frequency of the stimulus was 30° per cycle and the temporal frequency 1/6 Hz. This stimulus has previously been shown to robustly activate the visual cortex of the anesthetized monkey (Logothetis et al., 1999).

For the adaptation experiment, we used the following types of stimuli: an adapting stimulus and three types of test stimuli. The adapting stimulus consisted of a random pattern; that is, a rectangular area filled with 289 randomly oriented line segments. The test stimulus was either identical or different from the adapting stimulus. We used two types of test stimuli that differed from the adapting stimulus: a collinear pattern that was created by rotating 1/3 of the line segments of the adapting stimulus to generate a collinear shape (i.e., cube), and a random pattern that was created by rotating randomly the same line segments as in the collinear pattern to generate a random pattern different from the adapting stimulus. The average rotation angle of the line segments in the two test stimuli (collinear, random pattern) was the same. For each stimulus, we presented three rectangular patterns horizontally and three vertically to create a full field stimulus (30° horizontal × 23° vertical). This full field stimulus was flashed with a temporal frequency of 2/3 Hz. For all the stimuli, the size of the line segments was 0.25° and the distance between them was 0.25°. For a control adaptation experiment, we used similar stimuli of half of the size of the stimuli described above. We also used a different random pattern as the adapting stimulus and a different collinear pattern.

Design

For the localizer scans, we presented the rotating polar stimulus for 48 s followed by a 48 s background stimulation (gray full field stimulus at the average luminance of the polar stimulus). The direction of rotation of the polar stimulus was reversed every 5 s from clockwise to counterclockwise. This stimulus-blank sequence was repeated four times within a scan. We collected data from two localizer scans in each session to increase the power required for localizing the visual areas.

For the adaptation experiment, we used three stimulus conditions:

(1) identical random pattern, where the adapting and the test stimulus consisted of the same random pattern, (2) different random pattern, where the test stimulus was a different random pattern from the adapting stimulus, and (3) collinear pattern, where the test stimulus consisted of a collinear pattern embedded in a background of randomly oriented line segments. Fourteen to twenty trials for each condition were presented in each session. The presentation of trials across conditions was counterbalanced within each session. Each trial started with a 30 s background stimulation followed by the adapting random pattern for 150 s. A fast transient was introduced after the adapting stimulus by background stimulation of 86 ms and then the test stimulus was presented for 50 s followed by background stimulation of 30 s. For a control adaptation experiment, we used the same design except for shorter presentation time (50 s) for the adapting stimulus.

Imaging

Experiments were conducted in a vertical 4.7 Tesla scanner with a 40 cm diameter bore (Biospec 47/40v, Brucker Medical, Ettlingen, Germany). We used a custom chair and custom system for positioning the monkey within the magnet (Logothetis et al., 1999). During the localizer scans, we collected 13 horizontal slices using multi-shot (8) GE-recalled EPI images with a 128×128 matrix (1×1 mm^2 resolution, slice thickness 2 mm, TE = 20 ms, TR = 750 ms, FA = 40°). Three slices covering the occipitotemporal visual areas were then selected for the adaptation experiment. We followed similar fMRI data collection procedures with TR = 250 ms, FA = 20°–25° and multi-shot (4) GE-recalled EPI images used instead. Anatomical images were acquired using a matrix of 256×256 (0.5×0.5 mm resolution, inversion recovery-rapid acquisition with relaxation enhancement).

Data Analysis

fMRI data were processed using the BrainVoyager 4.6 software package. Preprocessing of all the functional data included temporal filtering of high frequencies and removal of linear trends. For each individual subject, we localized the visual areas that responded significantly more strongly ($p < 0.0032$, corrected) to the rotating polar stimulus than to the blank background stimulation as regions of interest. Statistical maps were calculated by correlating the signal time course with a boxcar reference function for each voxel based on the hemodynamic response properties (Boynton et al., 1996; Cohen, 1997; Dale and Buckner, 1997). The borders of the visual areas (V1, V2/V3, V4) were identified based on anatomical criteria (Gattass et al., 1981, 1988; Desimone and Ungerleider, 1986; Brewer et al., 2002). The ROIs were defined by the activated voxels within the anatomically defined areas. Voxels along the borders of these areas were excluded from the analysis due to possible partial volume effects. Similar procedure was followed when defining central and peripheral subregions in V1 and V2.

For each scan of the adaptation experiment, we computed the time course of the normalized fMRI response from the initial 30 s background stimulation period by averaging the data from all the voxels within each one of the independently defined ROIs in each of the five subjects. Then we averaged the data across trials and subjects for each experimental condition.

Human fMRI Studies

Subjects

Ten students from the University of Tuebingen participated in this study. The data from two subjects were excluded due to excessive head movement.

Stimuli

For the LOC localizer scans, we used grayscale (250×250 pixel or $10.9° \times 10.9°$) images of novel and familiar objects as well as scrambled versions of each set, as described previously (Kourtzi and Kanwisher, 2000).

For the localizer scans of the early retinotopic regions we used rotating triangular wedge stimuli for the mapping of the borders between visual areas and concentric rings for eccentricity mapping, as described in previous studies (Grill-Spector et al., 1998a). The subjects were required to fixate on the letter T that appeared in the center of the images and detect when it changed to an L. As described in previous studies (Kastner et al., 1997), this procedure controlled for fixation and attention of the subjects during the retinotopic scans.

For the adaptation scans, we used similar stimuli (random, collinear patterns) to those used for the monkey fMRI adaptation studies but they were rendered with Gabor elements as in previous studies (Kovacs and Julesz, 1993, 1994). The random patterns consisted of an area ($10.9° \times 10.9°$) filled with 144 randomly oriented Gabor elements. The collinear patterns were created by rotating 1/4 of the Gabor elements of the random patterns to generate collinear patterns that consisted of two concentric closed shapes ($6° \times 6°$) embedded in a field of randomly oriented Gabor elements. For all the stimuli, the size of the Gabor elements was 0.5° and the distance between them was 0.5°. We used 36 different closed shapes for the collinear patterns.

Design

Each subject was run in one session consisting of eight scans: two LOC localizer scans, two localizer scans for the early retinotopic areas, and four event-related scans for the adaptation experiment. The order of the scans was counterbalanced across subjects.

For the adaptation experiment, we used an event-related design (Dale and Buckner, 1997; Rosen et al., 1998) similar to previous studies (Kourtzi and Kanwisher, 2000, 2001). Each scan consisted of one epoch of experimental trials and two 8 s fixation epochs, one at the beginning and one at the end of the scan. Each scan consisted of 18 experimental trials for each of the four conditions tested and 18 fixation trials. Thus, a total of 108 trials were presented in each scan. A new trial began every 3 s and consisted of a pair of images presented sequentially. Each image was presented for 300 ms with a blank interval of 200 ms between images. A blank interval of 2200 ms was introduced between trials. As in previous studies (Kourtzi and Kanwisher, 2000, 2001), the order of presentation was counterbalanced so that trials from each condition, including the fixation condition, were preceded equally often by trials from each of the other conditions. Subjects were instructed to respond whether the two stimuli in a trial where the same or different, while fixating.

We used the following conditions that were defined by the type of stimuli presented in each trial: (1) identical random pattern, where the same random pattern was presented twice in a trial, (2) different random pattern, where 1/4 of the Gabor elements in the first stimulus in the trial were randomly rotated to generate a different random pattern that was presented as the second stimulus in the trial, and (3) random-to-collinear pattern, where the first stimulus in a trial was a random pattern while the second stimulus was a collinear pattern. The average rotation angle of the Gabor elements in the different random pattern and random-to-collinear pattern conditions was the same.

Imaging

For all the experiments, scanning was done on the 1.5 T Siemens scanner at the University Clinic in Tuebingen, Germany. A Gradient Echo pulse sequence (TR = 2 s, TE = 40 ms for the localizer scans; TR = 1 s, TE = 40 ms for the event-related scans) was used. Eleven axial slices (5 mm thick with 3.00×3.00 mm in-plane resolution) were collected with a head coil.

Data Analysis

fMRI data were processed using the BrainVoyager 4.6 software package. Preprocessing of all the functional data included head movement correction, temporal filtering of high frequencies, and removal of linear trends. The 2D functional images were aligned to 3D anatomical data and the complete data set was transformed to Tailarach coordinates inflated, unfolded, and flattened.

For each individual subject, the regions of interest (ROIs) defined were the LOC and the early retinotopic areas (V1, V2, VP, V3, V3a, V4v). 3D statistical maps were calculated for each one of these ROIs by correlating the signal time course with a reference function for each voxel based on the hemodynamic response properties (Boynton et al., 1996; Cohen, 1997; Dale and Buckner, 1997). For each individual subject, the LOC was defined as the set of continuous voxels in the ventral occipitotemporal cortex that showed significantly stronger activation ($p < 10^{-4}$, corrected) to intact than to scrambled images based on the average data from the two localizer scans. Two different regions in the LOC were identified: the lateral occipital region (LO) and the posterior fusiform (pFs) region as described in previous studies (e.g., Grill-Spector et al., 2000). Finally, the early visual areas (V1, V2, VP, V3, V3a, V4v) were identified based on standard retinotopic mapping procedures (Engel et al., 1994;

Sereno et al., 1995; DeYoe et al., 1996). Retinotopic borders between these regions were successfully identified for all but two subjects that were excluded from the analysis due to inconsistent fixation during the retinotopic scans. For areas V1 and V2, we identified central (up to 5°) and peripheral regions. Voxels along the borders of these regions were excluded from the analysis due to possible partial volume effects.

For each event-related adaptation scan, the fMRI response was extracted by averaging the data from all the voxels within each of the independently defined ROIs. In each scan, we averaged the signal intensity across all the trials in each condition at each of 11 corresponding time points (seconds) and converted these time courses to percent signal change relative to the fixation trials, as described previously (Kourtzi and Kanwisher, 2000, 2001). We then averaged the time courses for each condition across scans for each subject and then across subjects. Because of the hemodynamic lag in the fMRI response, the peak in overall response and therefore the differences across conditions are expected to occur at a lag of several seconds after stimulus onset (Boynton et al., 1996; Cohen, 1997; Dale and Buckner, 1997). To find the latencies at which any adaptation effects occurred, we conducted an ANOVA with factors of condition (identical random pattern, different random pattern, random-to-collinear pattern) and time point (measurements made at latencies of 0 through 10 s after trial onset) for each one of the ROIs. Significant main effects (after correction for temporal autocorrelation of the data) of condition (e.g., LOC [$F(1,154) = 18.63$, $p < 0.001$]), time (e.g., LOC [$F(10,154) = 22.67$, $p < 0.001$]), and a significant interaction effect [11 time points (e.g., LOC [$F(10,154) = 1.68$, $p < 0.05$])] verified that adaptation occurred and that it varied with latency. Follow-up contrast analyses run separately on each time point tested for a significantly lower response for the identical random pattern compared to the different random pattern and the random-to-collinear pattern conditions. This adaptation effect was found for each ROI only for time point 5 (e.g., LOC [$F(1,154) = 3.98$, $p < 0.05$]), and time point 6 (e.g., LOC [$F(1,154) = 5.38$, $p < 0.05$]), but not for the onset of a trial, i.e., time point 0 (e.g., LOC [$F(1,154) < 1$, $p = 0.40$]). Similar pattern or results were observed for the retinotopic regions. The average of the response at time points 5 and 6 was therefore taken as the measure of response magnitude for each condition in subsequent analyses.

Acknowledgments

We would like to thank the group of Wolfgang Grodd at the University Clinics in Tuebingen for providing the human MRI facilities and technical assistance with imaging. We would also like to thank the following people for helpful comments and suggestions: Constantinos Moutoussis, Natasha Sigala, and Stelios Smirnakis. This work was supported by the Max Planck Society, a McDonnell-Pew grant (#3944900) to Z.K., and a National Research Service Award from National Institutes of Health-National Eye Institute to A.S.T.

Received: October 15, 2002
Revised: December 3, 2002

References

Allman, J.M., Miezin, F., and McCuiness, E. (1985). Stimulus specific responses from beyond the classical receptive field: neurophysiological mechanisms for local-global comparisons in visual neurons. Annu. Rev. Neurosci. *8*, 407–430.

Bakin, J.S., Nakayama, K., and Gilbert, C.D. (2000). Visual responses in monkey areas V1 and V2 to three-dimensional surface configurations. J. Neurosci. *20*, 8188–8198.

Bar, M., Tootell, R.B.H., Schacter, D.L., Greve, D.N., Fischl, B., Mendola, J.D., Rosen, B.R., and Dale, A.M. (2001). Cortical mechanisms specific to explicit visual object recognition. Neuron *29*, 529–535.

Blakemore, C., and Tobin, E.A. (1972). Lateral inhibition between orientation detectors in the cat's visual cortex. Exp. Brain Res. *15*, 439–440.

Bosking, W.H., Zhang, Y., Schofield, B., and Fitzpatrick, D. (1997). Orientation selectivity and the arrangement of horizontal connections in tree shrew striate cortex. J. Neurosci. *17*, 2112–2127.

Boynton, G.M., Engel, S.A., Glover, G.H., and Heeger, D.J. (1996). Linear systems analysis of functional magnetic resonance imaging in human V1. J. Neurosci. *16*, 4207–4221.

Brewer, A.A., Press, W.A., Logothetis, N.K., and Wandell, B. (2002). Visual areas in macaque cortex measured using functional MRI. J. Neurosci. *22*, 10416–10426.

Buckner, R.L., Goodman, J., Burock, M., Rotte, M., Koutstaal, W., Schacter, D., Rosen, B., and Dale, A.M. (1998). Functional-anatomic correlates of object priming in humans revealed by rapid presentation event-related fMRI. Neuron *20*, 285–296.

Burkhalter, A., and Van Essen, D.C. (1986). Processing of color, form and disparity information in visual areas VP and V2 of ventral extrastriate cortex in the macaque monkey. J. Neurosci. *6*, 2327–2351.

Carandini, M., Barlow, H.B., O'Keefe, L.P., Poirson, A.B., and Movshon, J.A. (1997). Adaptation to contingencies in macaque primary visual cortex. Philos. Trans. R. Soc. Lond. B Biol. Sci. *352*, 1149–1154.

Cohen, M.S. (1997). Parametric analysis of fMRI data using linear systems methods. Neuroimage *6*, 93–103.

Dale, A.M., and Buckner, R.L. (1997). Selective averaging of rapidly presented individual trials using fMRI. Hum. Brain Mapp. *5*, 329–340.

Das, A., and Gilbert, C.D. (1997). Distortions of visuotopic map match orientation singularities in primary visual cortex. Nature *387*, 594–598.

Das, A., and Gilbert, C.D. (1999). Topography of contextual modulations mediated by short-range interactions in primary visual cortex. Nature *399*, 655–661.

DeAngelis, G.C., Robson, J.G., Ohzawa, I., and Freeman, R.D. (1992). Organization of suppression in receptive fields of neurons in cat visual cortex. J. Neurophysiol. *68*, 144–163.

DeAngelis, G.C., Freeman, R.D., and Ohzawa, I. (1994). Length and width tuning of neurons in the cat's primary visual cortex. J. Neurophysiol. *71*, 347–374.

Desimone, R., and Ungerleider, L.G. (1986). Multiple visual areas in the caudal superior temporal sulcus of the macaque. J. Comp. Neurol. *248*, 164–189.

DeYoe, E.A., Carman, G.J., Bandettini, P., Glickman, S., Wieser, J., Cox, R., Miller, D., and Neitz, J. (1996). Mapping striate and extrastriate visual areas in human cerebral cortex. Proc. Natl. Acad. Sci. USA *93*, 2382–2386.

Dobbins, A., Zucker, S.W., and Cynader, M.S. (1987). Endstopped neurons in the visual cortex as a substrate for calculating curvature. Nature *329*, 438–441.

Dragoi, V., Sharma, J., and Sur, M. (2000). Adaptation-induced plasticity of orientation tuning in adult visual cortex. Neuron *28*, 287–298.

Engel, S.A., Rumelhart, D.E., Wandell, B.A., Lee, A.T., Glover, G.H., Chichilnisky, E.J., and Shadlen, M.N. (1994). fMRI of human visual cortex. Nature *369*, 525.

Felleman, D.J., and Van Essen, D.C. (1987). Receptive field properties of neurons in area V3 of macaque monkey extrastriate cortex. J. Neurophysiol. *57*, 889–920.

Felleman, D.J., and Van Essen, D.C. (1991). Distributed hierarchical processing in the primate cerebral cortex. Cereb. Cortex *1*, 1–47.

Field, D.J., Hayes, A., and Hess, R.F. (1993). Contour integration by the human visual system: evidence for a local "association field." Vision Res. *33*, 173–193.

Fitzpatrick, D. (2000). Seeing beyond the receptive field in primary visual cortex. Curr. Opin. Neurobiol. *10*, 438–443.

Gattass, R., Gross, C.G., and Sandell, J.H. (1981). Visual topography of V2 in the macaque. J. Comp. Neurol. *201*, 519–539.

Gattass, R., Sousa, A.P., and Gross, C.G. (1988). Visuotopic organization and extent of V3 and V4 of the macaque. J. Neurosci. *8*, 1831–1845.

Gilbert, C.D. (1992). Horizontal integration and cortical dynamics. Neuron *9*, 1–13.

Gilbert, C.D. (1998). Adult cortical dynamics. Physiol. Rev. *78*, 467–485.

Gilbert, C.D., and Wiesel, T.N. (1989). Columnar specificity of intrinsic horizontal and corticocortical connections in cat visual cortex. J. Neurosci. *9*, 2432–2442.

Grill-Spector, K., and Malach, R. (2001). fMR-adaptation: a tool for studying the functional properties of human cortical neurons. Acta Psychol. (Amst.) *107*, 293–321.

Grill-Spector, K., Kushnir, T., Edelman, S., Itzchak, Y., and Malach, R. (1998a). Cue-invariant activation in object-related areas of the human occipital lobe. Neuron *21*, 191–202.

Grill-Spector, K., Kushnir, T., Hendler, T., Edelman, S., Itzchak, Y., and Malach, R. (1998b). A sequence of object-processing stages revealed by fMRI in the human occipital lobe. Hum. Brain Mapp. *6*, 316–328.

Grill-Spector, K., Kushnir, T., Edelman, S., Avidan, G., Itzchak, Y., and Malach, R. (1999). Differential processing of objects under various viewing conditions in the human lateral occipital complex. Neuron *24*, 187–203.

Grill-Spector, K., Kushnir, T., Hendler, T., and Malach, R. (2000). The dynamics of object-selective activation correlate with recognition performance in humans. Nat. Neurosci. *3*, 837–843.

Grinvald, A., Lieke, E.E., Frostig, R.D., and Hildesheim, R. (1994). Cortical point-spread function and long-range lateral interactions revealed by real-time optical imaging of macaque monkey primary visual cortex. J. Neurosci. *14*, 2545–2568.

Gross, C.G., Rocha-Miranda, C.E., and Bender, D.B. (1972). Visual properties of neurons in inferotemporal cortex of the macaque. J. Neurophysiol. *35*, 96–111.

Haxby, J.V., Gobbini, M.I., Furey, M.L., Ishai, A., Schouten, J.L., and Pietrini, P. (2001). Distributed and overlapping representations of faces and objects in ventral temporal cortex. Science *293*, 2425–2430.

Hess, R., and Field, D. (1999). Integration of contours: new insights. Trends Cogn. Sci. *3*, 480–486.

Hubel, D.H., and Wiesel, T.N. (1965). Receptive fields and functional architecture in two nonstriate visual areas (18 and 19) of the cat. J. Neurophysiol. *28*, 229–289.

Hubel, D.H., and Wiesel, T.N. (1968). Receptive fields and functional architecture of monkey striate cortex. J. Physiol. *195*, 215–243.

Kanwisher, N., Chun, M.M., McDermott, J., and Ledden, P.J. (1996). Functional imagining of human visual recognition. Brain Res. Cogn. Brain Res. *5*, 55–67.

Kapadia, M.K., Ito, M., Gilbert, C.D., and Westheimer, G. (1995). Improvement in visual sensitivity by changes in local context: parallel studies in human observers and in V1 of alert monkeys. Neuron *15*, 843–856.

Kapadia, M.K., Westheimer, G., and Gilbert, C.D. (1999). Dynamics of spatial summation in primary visual cortex of alert monkeys. Proc. Natl. Acad. Sci. USA *96*, 12073–12078.

Kastner, S., Nothdurft, H.C., and Pigarev, I.N. (1997). Neuronal correlates of pop-out in cat striate cortex. Vision Res. *37*, 371–376.

Knierim, J.J., and van Essen, D.C. (1992). Neuronal responses to static texture patterns in area V1 of the alert macaque monkey. J. Neurophysiol. *67*, 961–980.

Kofka, K. (1935). Principles of Gestalt Psychology (New York: Harcourt).

Kourtzi, Z., and Kanwisher, N. (2000). Cortical regions involved in perceiving object shape. J. Neurosci. *20*, 3310–3318.

Kourtzi, Z., and Kanwisher, N. (2001). Representation of perceived object shape by the human lateral occipital complex. Science *293*, 1506–1509.

Kovacs, I., and Julesz, B. (1993). A closed curve is much more than an incomplete one: effect of closure in figure-ground segmentation. Proc. Natl. Acad. Sci. USA *90*, 7495–7497.

Kovacs, I., and Julesz, B. (1994). Perceptual sensitivity maps within globally defined visual shapes. Nature *370*, 644–646.

Lamme, V.A. (1995). The neurophysiology of figure-ground segregation in primary visual cortex. J. Neurosci. *15*, 1605–1615.

Lamme, V.A., and Roelfsema, P.R. (2000). The distinct modes of vision offered by feedforward and recurrent processing. Trends Neurosci. *23*, 571–579.

Lamme, V.A., Super, H., and Spekreijse, H. (1998). Feedforward, horizontal, and feedback processing in the visual cortex. Curr. Opin. Neurobiol. *8*, 529–535.

Lamme, V.A., Rodriguez-Rodriguez, V., and Spekreijse, H. (1999). Separate processing dynamics for texture elements, boundaries and surfaces in primary visual cortex of the macaque monkey. Cereb. Cortex *9*, 406–413.

Lee, T.S., and Nguyen, M. (2001). Dynamics of subjective contour formation in the early visual cortex. Proc. Natl. Acad. Sci. USA *98*, 1907–1911.

Lee, T.S., Mumford, D., Romero, R., and Lamme, V.A. (1998). The role of the primary visual cortex in higher level vision. Vision Res. *38*, 2429–2454.

Lerner, Y., Hendler, T., Ben-Bashat, D., Harel, M., and Malach, R. (2001). A hierarchical axis of object processing stages in the human visual cortex. Cereb. Cortex *11*, 287–297.

Lerner, Y., Hendler, T., and Malach, R. (2002). Object-completion effects in the human lateral occipital temporal complex. Cereb. Cortex *12*, 163–177.

Li, W., Their, P., and Wehrhahn, C. (2000). Contextual influence on orientation discrimination of humans and responses of neurons in V1 of alert monkeys. J. Neurophysiol. *83*, 941–954.

Lisberger, S.G., and Movshon, J.A. (1999). Visual motion analysis for pursuit eye movements in area MT of macaque monkeys. J. Neurosci. *19*, 2224–2246.

Logothetis, N.K., and Sheinberg, D.L. (1996). Visual object recognition. Annu. Rev. Neurosci. *19*, 577–621.

Logothetis, N.K., Guggenberger, H., Peled, S., and Pauls, J. (1999). Functional imaging of the monkey brain. Nat. Neurosci. *2*, 555–562.

Logothetis, N.K., Pauls, J., Augath, M., Trinath, T., and Oeltermann, A. (2001). Neurophysiological investigation of the basis of the fMRI signal. Nature *412*, 150–157.

MacEvoy, S.P., Kim, W., and Paradiso, M.A. (1998). Integration of surface information in primary visual cortex. Nat. Neurosci. *1*, 616–620.

Maffei, L., and Fiorentini, A. (1976). The unresponsive region of visual cortical receptive fields. Vision Res. *16*, 1131–1139.

Malach, R., Amir, Y., Harel, M., and Grinvald, A. (1993). Relationship between intrinsic connections and functional architecture revealed by optical imaging and in vivo targeted biocytin injections in primate striate cortex. Proc. Natl. Acad. Sci. USA *90*, 10469–10473.

Malach, R., Reppas, J.B., Benson, R.B., Kwong, K.K., Jiang, H., Kennedy, W.A., Ledden, P.J., Brady, T.J., Rosen, B.R., and Tootell, R.B.H. (1995). Object-related activity revealed by functional magnetic resonance imaging in human occipital cortex. Proc. Natl. Acad. Sci. USA *92*, 8135–8138.

Mareschal, I., Sceniak, M.P., and Shapley, R.M. (2001). Contextual influences on orientation discrimination: binding local and global cues. Vision Res. *41*, 1915–1930.

Maunsell, J.H.R., and Newsome, W.T. (1987). Visual processing in monkey extrastriate cortex. Annu. Rev. Neurosci. *10*, 363–401.

Mendola, J.D., Dale, A.M., Fischl, B., Liu, A.K., and Tootell, R.B.H. (1999). The representation of real and illusory contours in human cortical visual areas revealed by fMRI. J. Neurosci. *19*, 8560–8572.

Miller, E.K., Li, L., and Desimone, R. (1991). A neural mechanism for working memory and recognition memory in inferior temporal cortex. Science *254*, 1377–1379.

Miller, E.K., Erikson, C.A., and Desimone, R. (1996). Neural mechanisms of visual working memory in prefrontal cortex of the macaque. J. Neurosci. *16*, 5154–5167.

Moller, P., and Hurlbert, A.C. (1996). Psychophysical evidence for fast region-based segmentation processes in motion and color. Proc. Natl. Acad. Sci. USA *93*, 7421–7426.

Movshon, J.A., and Lennie, P. (1979). Pattern-selective adaptation in visual cortical neurons. Nature *278*, 850–852.

Mueller, J.R., Metha, A.B., Krauskopf, J., and Lennie, P. (1999). Rapid adaptation in visual cortex to the structure of images. Science *285*, 1405–1408.

Nakayama, K., and Shimojo, S. (1992). Experiencing and perceiving visual surfaces. Science *257*, 1357–1363.

Nothdurft, H.C., Gallant, J.L., and Van Essen, D.C. (1999). Response modulation by texture surround in primate area V1: correlates of "popout" under anesthesia. Vis. Neurosci. *16*, 15–34.

Nothdurft, H.C., Gallant, J.L., and Van Essen, D.C. (2000). Response profiles to texture border patterns in area V1. Vis. Neurosci. *17*, 421–436.

Paradiso, M.A., and Nakayama, K. (1991). Brightness perception and filling-in. Vision Res. *31*, 1221–1236.

Peterhans, E., and von der Heydt, R. (1989). Mechanisms of contour perception in monkey visual cortex. II. Contours bridging gaps. J. Neurosci. *9*, 1749–1763.

Polat, U. (1999). Functional architecture of long-range perceptual interactions. Spat. Vis. *12*, 143–162.

Polat, U., and Bonneh, Y. (2000). Collinear interactions and contour integration. Spat. Vis. *13*, 393–401.

Polat, U., and Sagi, D. (1993). Lateral interactions between spatial channels: suppression and facilitation revealed by lateral masking experiments. Vision Res. *33*, 993–999.

Polat, U., and Sagi, D. (1994). The architecture of perceptual spatial interactions. Vision Res. *34*, 73–78.

Polat, U., Mizobe, K., Pettet, M.W., Kasamatsu, T., and Norcia, A.M. (1998). Collinear stimuli regulate visual responses depending on cell's contrast threshold. Nature *391*, 580–584.

Rosen, B.R., Buckner, R.L., and Dale, A.M. (1998). Event-related functional MRI: past, present, and future. Proc. Natl. Acad. Sci. USA *95*, 773–780.

Rossi, A.F., Rittenhouse, C.D., and Paradiso, M.A. (1996). The representation of brightness in primary visual cortex. Science *273*, 1104–1107.

Rossi, A.F., Desimone, R., and Ungerleider, L.G. (2001). Contextual modulation in primary visual cortex of macaques. J. Neurosci. *21*, 1698–1709.

Salin, P.A., and Bullier, J. (1995). Corticocortical connections in the visual system: structure and function. Physiol. Rev. *75*, 107–154.

Sceniak, M.P., Ringach, D.L., Hawken, M.J., and Shapley, R. (1999). Contrast's effect on spatial summation by macaque V1 neurons. Nat. Neurosci. *2*, 733–739.

Sengpiel, F., Sen, A., and Blakemore, C. (1997). Characteristics of surround inhibition in cat area 17. Exp. Brain Res. *116*, 216–228.

Sereno, M.I., Dale, A.M., Reppas, J.B., Kwong, K.K., Belliveau, J.W., Brady, T.J., Rosen, B.R., and Tootell, R.B.H. (1995). Borders of multiple visual areas in humans revealed by functional magnetic resonance imaging. Science *268*, 889–893.

Smith, A.T., Singh, K.D., Williams, A.L., and Greenlee, M.W. (2001). Estimating receptive field size from fMRI data in human striate and extrastriate visual cortex. Cereb. Cortex *11*, 1182–1190.

Smith, M.A., Bair, W., and Movshon, J.A. (2002). Signals in macaque striate cortical neurons that support the perception of glass patterns. J. Neurosci. *15*, 8334–8345.

Tanaka, K. (1996). Inferotemporal cortex and object vision. Annu. Rev. Neurosci. *19*, 109–139.

Tolias, A.S., Smirnakis, S.M., Augath, M.A., Trinath, T., and Logothetis, N.K. (2001). Motion processing in the macaque: revisited with functional magnetic resonance imaging. J. Neurosci. *21*, 8594–8601.

Wandell, B.A. (1999). Computational neuroimaging of human visual cortex. Annu. Rev. Neurosci. *22*, 145–173.

Van Essen, D.C., Anderson, C.H., and Felleman, D.J. (1992). Information processing in the primate visual system: an integrated systems perspective. Science *255*, 419–423.

von der Heydt, R., and Peterhans, E. (1989). Mechanisms of contour perception in monkey visual cortex. I. Lines of pattern discontinuity. J. Neurosci. *9*, 1731–1748.

Zenger, B., and Sagi, D. (1996). Isolating excitatory and inhibitory nonlinear spatial interactions involved in contrast detection. Vision Res. *36*, 2497–2513.

Zhou, H., Friedman, H.S., and von der Heydt, R. (2000). Coding of border ownership in monkey visual cortex. J. Neurosci. *20*, 6594–6611.

Zipser, K., Lamme, V.A., and Schiller, P.H. (1996). Contextual modulation in primary visual cortex. J. Neurosci. *16*, 7376–7389.